Establishment and genetic characterization of ANGM-CSS, a novel, immortal cell line derived from a human glioblastoma multiforme

ANGELANTONIO NOTARANGELO[1*], DOMENICO TROMBETTA[2*], VINCENZO D'ANGELO[5], PAOLA PARRELLA[2], ORAZIO PALUMBO[1], CLELIA TIZIANA STORLAZZI[3], LUCIANA IMPERA[3], LUCIA ANNA MUSCARELLA[2], ANTONELLA LA TORRE[2], ANDREA AFFUSO[4], VITO MICHELE FAZIO[2], MASSIMO CARELLA[1] and LEOPOLDO ZELANTE[1]

[1]Medical Genetics Unit, [2]Laboratory of Oncology, IRCCS Casa Sollievo della Sofferenza Hospital, I-71013 San Giovanni Rotondo (FG); [3]Department of Biology, University of Bari Aldo Moro, I-70125 Bari; [4]Biogem IRGS, I-83031 Ariano Irpino (AV); [5]Department of Neurosurgery, IRCCS Casa Sollievo della Sofferenza Hospital, I-71013 San Giovanni Rotondo (FG), Italy

Received September 27, 2013; Accepted October 15, 2013

DOI: 10.3892/ijo.2013.2224

Abstract. Glioblastoma multiforme (World Health Organization, grade IV astrocytoma) is the most common and most aggressive malignant primary brain tumor. We report a novel cell line, designated as ANGM-CSS, which was established from a 56-year-old male patient with a surgically removed glioblastoma multiforme. The ANGM-CSS cell line was established *in vitro* and characterized using histological and immunohistochemical staining, classical and molecular cytogenetic analyses, molecular studies and functional assays using a xenograft model in immunodeficient animals. ANGM-CSS was positive for CD133, nestin and vimentin proteins, whereas GFAP showed staining only in a fraction of the cells. Cytogenetic and molecular cytogenetic analysis revealed a near-tetraploid karyotype, with a modal chromosome number from 88 to 91, and additional cytogenetic abnormalities, such as the t(6;14)(p12;q11.2), t(8;10)(q24.2;q21.1) and t(5;9)(q34;p21) unbalanced translocations. Moreover, ANGM-CSS showed amplification of the *MET* and *EGFR* genes whose overexpression was observed at the mRNA level. Interestingly, ANGM-CSS is tumorigenic when implanted in immunodeficient mice, and the cells obtained from the xenografts showed the same morphology and karyotype *in vitro* as the original cell line. ANGM-CSS represents a biologically relevant cell line to be used to investigate the molecular pathology of glioblastoma multiforme, also to evaluate the efficacy of novel therapeutic drugs *in vitro*.

Correspondence to: Dr Domenico Trombetta, Laboratory of Oncology, IRCCS Casa Sollievo della Sofferenza Hospital, Viale Cappuccini, I-71013 San Giovanni Rotondo (FG), Italy
E-mail: d.trombetta@operapadrepio.it

*Contributed equally

Key words: glioblastoma cell line, cytogenetics, fluorescent *in situ* hybridization, *in vitro* test system

Introduction

Glioma is the most common primary brain tumor affecting yearly 3-5/100,000 and occurring mainly in adults >45 years old (1-3). The ability of glioma to invade and infiltrate diffusely contiguous brain tissue limits the complete surgical resection and the efficacy of standard therapies (4). Glioblastoma multiforme (GBM), a grade IV astrocytoma as currently defined by the World Health Organization (WHO) classification (5), is the most common and the most lethal form of brain tumor. The therapeutic approach against this tumor consists in surgical resection followed by radiation and chemotherapy with temozolomide (TMZ) (6,7). At present, such treatment can only slightly modify the patient's outcome. In fact, the tumor typically recurs after an average of only 6.9 months, resulting in a median survival rate of <1 year following diagnosis (8). Permanent cell lines represent important tools to study the behaviour of human tumors, such as their growth and metabolism, drug sensitivity and resistance, as well as genomic and expression profiles (9-11). Furthermore, some cultivated cancer cells can originate a novel tumor when transplanted into nude mice, providing an experimental system to test potential novel therapeutic drugs (12). Here we report the establishment and the characterization, by cytogenetic and molecular approaches, of a novel cell line termed as ANGM-CSS, derived from a patient with GBM.

Materials and methods

Patient history. The patient was a 56-year-old male, surgically treated to remove a large primary tumor localized in the left temporo-occipital lobe with invasion of the ventricular cornus (Fig. 1A). Hematoxylin and eosin staining (Fig. 1B) and immunohistochemical examination for GFAP, α-SMA and HMB45 were performed as part of the routine assessment of tumor type/phenotype. Immunostaining demonstrated a weak positivity for GFAP (Fig. 1C) but was negative for α-SMA and HMB45 (data not shown). The final diagnosis was GBM with spindle, mitotically active cells showing a fascicular growth pattern.

After surgery, the patient was treated with temozolomide at a daily dose of 75 mg/m^2 of body surface in association with fractionated radiotherapy (60 Gy) for 6-7 weeks. The patient died 18 months after surgery.

Establishment of primary culture. After surgical removal, upon institutional Ethics Committee approval, the tumor specimen was placed immediately in DMEM-F12 medium without serum, repeatedly washed with phosphate-buffered saline (PBS, Invitrogen, Carlsbad, CA, USA) and then placed in a 30-mm Petri dish. The specimen was cut in 1-2 mm or tinier fragments and transferred in a poly-D-lysine treated flask with a small amount of Dulbecco's modified Eagle's medium/F12 medium (D-MEM/F12, Invitrogen) (1:1, v/v) supplemented with 10% fetal bovine serum (FBS, Invitrogen), 100 U/ml penicillin and 100 μg/ml streptomycin (PenStrep, Invitrogen) in order to allow the fragments to adhere to the surface of the flask. Primary culture was incubated at 37˚C in 5% CO_2 humidified atmosphere, and 5 ml of complete medium was added 24 h later. After one week, the primary culture was washed with PBS to remove non-adherent fragments and fresh medium prewarmed at 37˚C was added. These procedures were repeated every 3 days until primary culture reached local confluence. Then cells were treated with 0.05% trypsin (Invitrogen) and 0.02% EDTA (Invitrogen), washed with PBS and transferred into a T-75 flask without biocoat and containing complete medium DMEM/F12. Next, the culture was serially transferred by using the same procedures once or twice a week. Every 10 passages, one amount of cells was counted with Z1-Coulter (IL-Laboratories). Cells ($50x10^6$) were frozen in medium with 10% dimethyl sulfoxide (DMSO) and stored in liquid nitrogen. Cells were propagated by serial passages (split ratio 1:3) along 2 years, until 105th passage. Growth curves were established at the 32nd passages by seeding $1x10^5$ cells into three 35-mm culture dishes. Triplicate dishes were harvested and counted daily with Z1-Coulter (IL-Laboratories). The cell number was determined as the average number of cells ± SD in each time interval.

Immunophenotypical characterization of ANGM-CSS cell line. Immunofluorescence analysis was performed at different passages to establish GFAP, nestin, CD133 and vimentin localization in the ANGM cell cultures. After trypsin treatment, 10^5 cells were seeded on 20x20 mm coverslips, rinsed twice in PBS, and fixed in PBS containing 4% formaldehyde (pH 7.2-7.4) for 10 min at room temperature (RT), washed for 10 min three times with PBS, permeabilized with PBS/0.2% Triton X-100 (MP Biomedical) and blocked for 30 min with PBS containing bovine serum albumin (BSA). After three washings with PBS, the cells were incubated with a primary antibody against CD133 (AP2010b, purified rabbit, ABGENT), nestin (sc-23927, mouse monoclonal IgG_1, Santa Cruz Biotechnology), vimentin (sc-6260, mouse monoclonal IgG_1, Santa Cruz Biotechnology), GFAP (sc-58766, mouse monoclonal IgG_1, Santa Cruz Biotechnology) diluted 1:300 in BSA for 1 h at RT. After extensive washing in PBS, the coverslips were incubated with the secondary antibodies for 30 min at room temperature. A goat anti-mouse IgG-FITC conjugated (sc-2010, 1:200, Santa Cruz Biotechnology) for vimentin, nestin and GFAP, and a goat anti-rabbit Ig-G FITC conjugated (sc-2012, 1:200, Santa Cruz Biotechnology) for CD-133 were used as secondary antibodies. Nuclei were then washed only once with PBS and stained with DAPI (1 mg/ml). The fluorescent staining was visualized using Nikon E1000 microscopy.

Cytogenetic analysis. ANGM-CSS cells were subcultured at passages 5, 32, 67, 86 and incubated overnight with Colcemid (0.05 mg/ml, Invitrogen). Cells were dispersed with 0.5% trypsin (Invitrogen) and 0.02 EDTA (Invitrogen), then washed with 1X PBS and treated with 0.075 M KCl hypotonic solution and fetal bovine serum (1:1, v/v) for 20 min at 37˚C. The cells were then fixed with methanol:acetic acid (3:1, v/v) solution and stored for 1 h at -20˚C. Cell suspension were dropped on ice glass slides and stained in Giemsa stain after banding with GAG-acid solution at 55˚C. Karyotyping was performed by use of the Genikon software (Nikon Italia, Firenze, Italy) and described in accordance to the International System for Human Cytogenetic Nomenclature (ISCN 2009).

SNP array analysis. SNP array experiments and data analysis were performed using the Genome-Wide Human SNP 6.0 array (Affymetrix, Santa Clara, CA, USA) as previously described (13).

Multicolor fluorescence in situ hybridization (M-FISH). M-FISH analysis of ANGM-CSS cells was performed using the commercially available 24-colour SpectraVysion probe (Abbott), according to the manufacturer's instructions. Metaphase images were captured using a Leica DM-RXA2 epifluorescence microscope equipped with an 8-position automated filter wheel and a cooled CCD camera (Princeton Instruments). Six fluorescent images per metaphase were captured using filter combinations specific for SpectrumGold, SpectrumAqua, SpectrumGreen, FRed, Red, and DAPI. Images were processed using the Leica CW4000 M-FISH software.

FISH. BAC clones for FISH analysis were selected according to the March 2006 release of the UCSC Human Genome Browser (http://genome.ucsc.edu) (data not shown). FISH experiments were carried out as previously described (14).

Quantitative reverse transcription polymerase chain reaction (RTq-PCR). Expression analysis of *EGFR* and *MET* genes was performed comparing the mRNA levels in the ANGM-CSS cell line and normal human astrocytes (NHA) (Lonza Walkersville, MD, USA) by QRT-PCR on 7700 sequence detection system (Applied Biosystems, Foster City, CA, USA) using MGB TaqMan chemistry and the $2^{-\Delta Ct}$ relative method for relative quantification (15). For the analysis were used the following TaqMan® Gene Expression Assays (Applied Biosystems): *MET* (Hs01565580_m1) and *EGFR* (Hs01076092_m1). The human large ribosomal protein transcript (Human *RPLP09*, Applied Biosystems) was used as endogenous control.

Quantitative methylation-specific PCR (QMSP) for the MGMT gene. DNA extracted from ANGM-CSS underwent bisulfite treatment and subsequent DNA purification using the Epitect Bisulfate kit (Qiagen Sci, MD, USA) according to the manu-

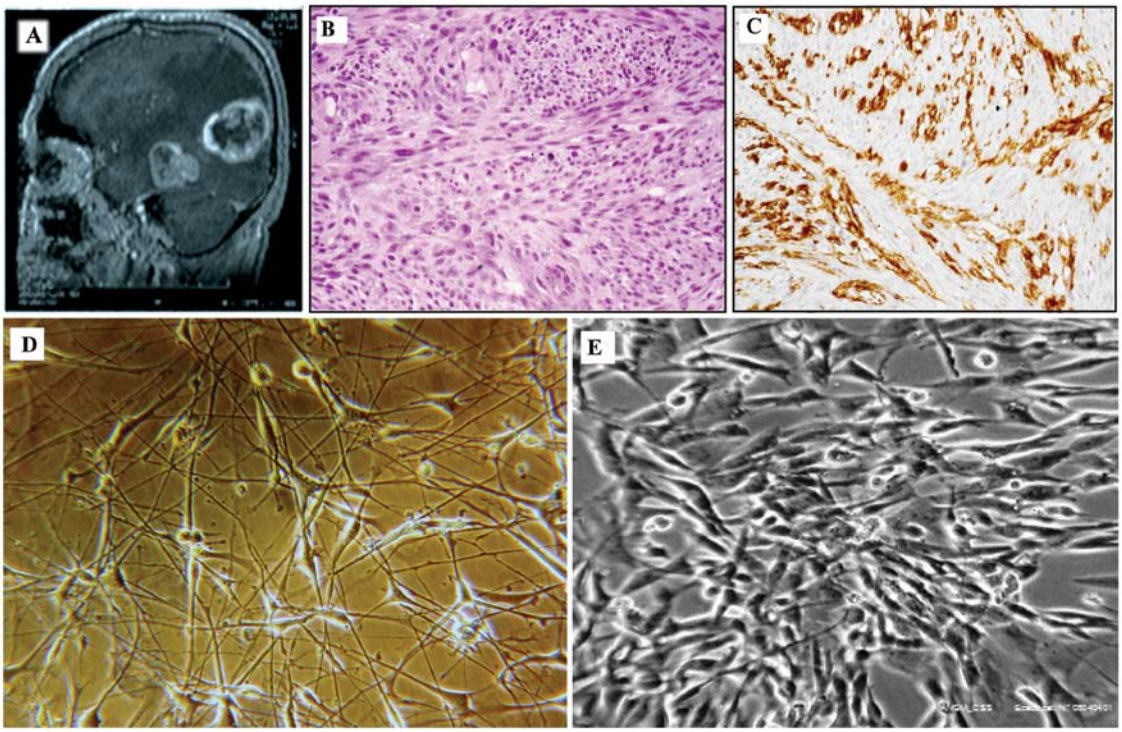

Figure 1. Morphological characteristics of the primary tumor and ANGM-CSS cell line. (A) Enhanced MRI before surgery showing a large temporo-occipital lesion heterogeneous lesion mostly necrotic with a marked edema suggestive of a glioma. (B) Histological section (stained with hematoxylin-eosin) of GBM (x100 original magnification), showing high cellular density and formation of fascicular grown pattern. (C) Micrograph of the tumor section showing strong immunoreactivity for GFAP. (D) Micrograph of the cultured ANGM-CSS cells (32nd passage) at x40 original magnification (phase-contrast). (E) Morphology of ANGM-CSS cells subcultivated from nude mice at x40 original magnification (phase-contrast).

facturer's instructions. Bisulphite converted DNA was used as template for fluorescence-based real-time QMSP. Real-time PCR experiments for *MGMT* were performed as previously described (16).

TP53 and KRAS mutation analysis. PCR amplifications of *KRAS* gene exon 2 and *TP53* gene exons 4-8 were performed as previously described (17). Amplification reactions were performed in a GeneAmp PCR System 9700 (Perkin-Elmer, Foster City, CA, USA) in a final reaction volume of 25 μl containing 100 ng of genomic DNA template, 0.25 nM dNTPs, 20 pmol of each primers, 1 U HotMaster Taq polymerase (Eppendorf), in 1X PCR reaction buffer. All PCR products were purified using GFX™ PCR DNA and Gel Band Purification kit (GE Healthcare, Buckinghamshire, UK) and sequenced. Sequencing reactions were performed in 10 μl of final volume using 3 pmol of primer, 4-6 ng of DNA template and 1 μl of Big Dye Terminator Ready Reaction mix v.1.1 (Applied Biosystems). Sequencing reactions were loaded on an ABI 3100 capillary sequencer (Applied Biosystems) and by the Sequencing Analysis software v.3.7 (PE Applied Biosystems).

FIG-ROS1 and FGFR3-TACC3 fusion gene detection. Total RNA was isolated from ANGM-CSS cell line using the TRIzol reagent (Invitrogen™ Life Technologies, Carlsbad, CA, USA) according to the manufacturer's instructions. The Agilent 2100 Bioanalyzer was used to measure the quantity, integrity and purity of total RNA. RNA (1 μg) was reverse transcribed by High Capacity cDNA Reverse Transcription kit (Life Technologies) according to the manufacturer's instructions. To detect the possible presence of *FIG-ROS1* fusion transcript, reverse transcriptase (RT)-PCR experiments were performed using primers previously reported (18). The detection of the *FGFR3-TACC3* fusion gene was performed on the basis of the results previously described (19) and using the primers TACC3_Ex5_f (CTTGAACTCTGCCAGCACCT) and FGFR3_Ex16_r GTGGGCAAACACGGAGTC. Briefly, for both chimeric genes, 2 μl cDNA was used as template in a final volume of 50 μl containing 10X PCR buffer, 0.25 mM of each dNTP, 0.5 μM of each forward and reverse primer, 0.5 U HotMaster Taq DNA polymerase (5Prime). The PCRs were run on a GeneAmp PCR System 9700 (Applied Biosystem) with the cycling profile of initial denaturation for 2 min at 94˚C followed by 35 cycles of 1 min at 94˚C, 1 min at 56˚C and 2 min at 72˚C, with a final extension for 10 min at 72˚C. For the experiments for *FIG-ROS1* detection, the cDNA of U118MG cell line was used as positive control (18-20). The PCR product (20 μl) was analyzed by electrophoresis through a 1% agarose gel containing ethidium bromide for staining.

Murine xenograft model. Six female, 6-week old athymic nude mice (Crl:CD1-NU-*Foxn1*^{nu} from Charles River Laboratories, Italy) were used for transplantation studies in accordance with national and institutional guidelines and were kept under specific pathogen-free (SPF) conditions. The mice were inoculated subcutaneously with 200 μl of cell suspension at four different concentrations (from a minimum concentration of $5x10^5$ cells in 200 μl of mixture PBS/Matrigel 1:1, to a

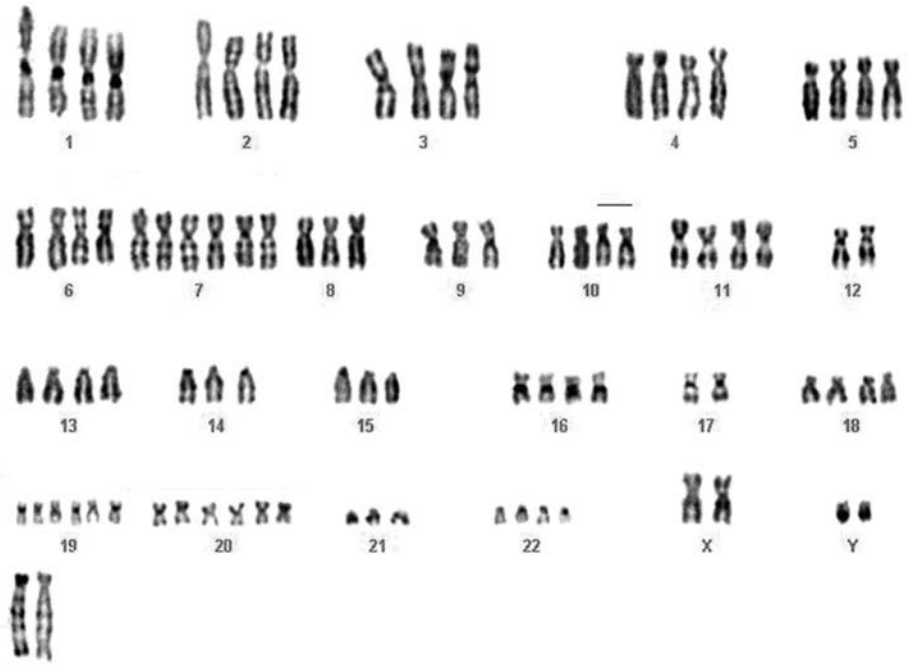

Figure 2. G-banding analysis of long-term cultured cells from the ANGM-CSS.

Table I. Comparison between the genetic abnormalities reported by the Cancer Genome Atlas (TCGC) research network at gene loci critically involved in gliomas and gains and losses detected in ANGM-CSS cell line by SNP array analysis.[a]

Gene	Locus	TCGA[b]	ANGM-CSS
Genes involved in RTK/RAS/PI-3K signaling			
EGFR	7p12.3-p12.1	Amplified	45% amplified
ERBB2	17q21.1	Mutated	8% homozygous deletion
PDGFRA	4q12	Amplified	13% no change
MET	7q31	Amplified	4% amplified
NF1	17q11.2	Homozygous deletion	18% homozygous deletion
RAS	6p21.3	Mutated	2% no change
PI3K	3q26.3	Mutated	15% no change
PTEN	10q23.31	Homozygous deletion	36% homozygous deletion
AKT	14q32.3	Amplified	2% no change
FOXO	6q21	Mutated	1% homozygous deletion
TP53 regulation			
CDKN2A	9p21	Homozygous deletion	49% deleted Hom
MDM2	12q14.3-q15	Amplified	14% amplified
MDM4	1q32	Amplified	7% no change
TP53	17p13.1	Homozygous deletion	35% no change
RB signaling			
CDKN2A	9p21	Homozygous deletion	52% homozygous deletion
CDKN2B	9p21	Homozygous deletion	47% homozygous deletion
CDKN2C	1p32	Homozygous deletion	2% no change
CDK4	12q14	Amplified	18% amplified
CCND2	12p13	Amplified	2% amplified
CDK6	7q21-22	Amplified	1% amplified
RB1	13q14.1-q14.2	Homozygous deletion	11% homozygous deletion

[a]The ANGM-CSS cell line is characterized by amplification of the *EGFR, MET, MDM2, CDK4* and *CDK6* genes and homozygous deletion of *NF1, CDKN2A* and *CDKN2B* genes. [b]TCGA, The Cancer Genome Atlas.

Table II. SNP array results.

Chromosome	Gain (chromosome/cytoband)	Loss (chromosome/cytoband)
2		2p11.2
3		3q13.31-3q13.32, 3q13.31
4		4q34.3
5	5q34-5q35.3,	5q34, 5q34
6		6q16.3-6q27, 6q11.1-6q16.2
7	7, 7p22.3-7q36.3	
9		9p24.2, 9p24.3-9p24.2, 9p24.2-9p21.1
10		10, 10q23.1, 10p15.3-10q23.1, 10q23.1-10q26.3
12	12q24.23-12q24.31, 12q24.32, 12q22-12q23.1, 12q14.1-12q21.1, 12q24.12-12q24.13, 12q23.1, 12q23.1-12q23.2, 12q13.2-12q13.3, 12q24.31, 12q24.13, 12q23.3, 12q13.3-12q14.1	12q12, 12q23.1, 12q21.1, 12q23.1, 12q23.1, 12q23.2-12q23.3, 12q21.1-12q22, 12q23.3-12q24.12, 12q24.13-12q24.23, 12q14.1, 12q24.32-12q24.33
14	14q11.2	14
17	17p13.1, 17p13.2, 17p13.3	17q11.1-17q21.31
19	19, 19p13.3-19q13.43	
20	20, 20p13-20q13.33	
21		21
X		Xp22.33-Xq28

maximum concentration of $10x10^6$ cells in 200 μl of mixture PBS/Matrigel 1:1). Mice were bilaterally inoculated on the flank (three injections for each concentration), while a control mouse was inoculated with Matrigel. The tumor diameter was measured weekly with a digital caliper and the tumor volume (mm^3) was calculated as previously described (21). All mice used in the experiment were monitored daily for signs of suffering and to identify cases of spontaneous death.

Results

The primary culture grew initially slowly, reaching cell confluence three weeks after surgical removal. Analysis by phase contrast microscopy showed a mixed population with dendritic-like and spindle cells (Fig. 1D). From the 26th passage, the cells showed a spindle shape with large nuclei. Cells were propagated until the 105th passage, growing continuously for >2 years, without morphological changes. The doubling time was calculated at the 32nd passage. One day after subculturing, the cells entered an exponential growth phase, where the doubling time was ~60 h. Immunofluorescence analysis showed a decrease in GFAP immunoreactivity, starting from the 17th passage to completely disappear during further serial passages *in vitro*. The cells were persistently positive for vimentin and nestin, while only a small fraction of the ANGM-CSS cell population showed a CD133 staining (data not shown). Cytogenetic and molecular analyses were performed at the 32nd, at the 70th and at the last passages. Metaphase spreads from long-term cultured cells were treated by conventional cytogenetic methods for karyotype analysis and thirty-two metaphases were analyzed. The cytogenetic analysis showed a strong karyotypic complexity and heterogeneity; the chromosome number was near-tetraploid and in addition to whole chromosome losses (chromosomes 10, 14 and 21) and gains (chromosomes 7, 20 and 19), two clonal chromosomal translocations were observed: a t(6;14)(p12;q11.2), and a t(8;10)(q24.2;q21.1). Moreover, the recurrent deletion of the long arm of chromosome 6 was detected and one marker chromosome apparently composed of chromosome 12 material [mar(12)] was found to be recurrent in 100% of the cell population (Fig. 2). According to the 2009 recommendations of the International System for Human Cytogenetic Nomenclature (22), the karyotype was described as follows: 88~91,XXYY,-6,+7,del(9)(p21.1)x2,-10,-12,+der(14)t(6;14)(p12;q11.2)x2,-17, +19,+20,-21, +marx2[cp32].

To better define genomic gains and losses, SNP array analysis was performed on DNA extracted at the same passages. The SNP analysis confirmed the high genomic complexity, showing, in addition to the losses and gains of whole chromosomes detected by chromosome banding, the deletion of the 6q, copy number alterations at 5q (gain of a 14.6 Mb region from 5q34 to 5qter) and 9p (loss of a 28.7-Mb segment from 9p24.3 to 9p21.1); in addition, chromosome 12 showed copy number changes from 10 to 1 along its long arm (Fig. 3A), similarly to regions of chromosomes 7, 16 and 17. The overall SNP array results are listed in Table II.

M-FISH analysis confirmed the presence of the unbalanced translocation der(14)t(6;14)(p12;q11.2) and detected two addi-

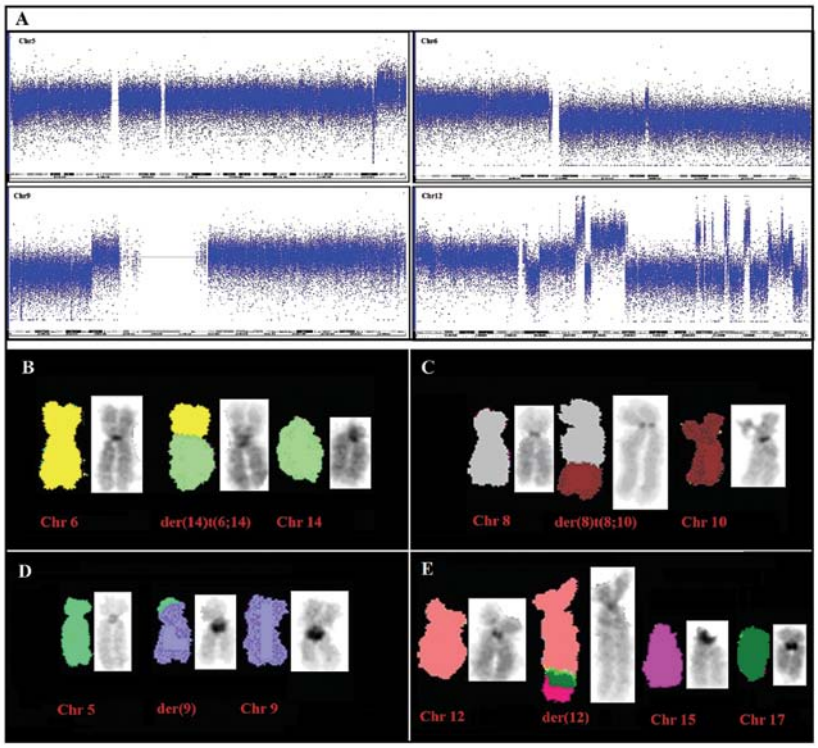

Figure 3. (A) SNP array analysis showing gains and losses relating to chromosomes 5, 6, 9 and 12. (B-E) M-FISH results (partial metaphases) showing the rearragements between chr6 and 14 (B), chr8 and 10 (C), chr5 and 9 (D). The M-FISH clarified the structure of mar(12), arising from a complex rearrangement between chr12 and amplified region from chr15 and 17 (E).

tional unbalanced translocations: der(8)t(8;10)(q24.2;q21.1) and der(9)t(5;9)(q34;p21), in agreement with the SNP array data and clarified that the additional material on der(12), already detected by G-banding and SNP-array CGH, originated from amplified material from chromosomes 7, 12 and 17 (Fig. 3B-E). Chromosome aberrations detected by both SNP array and M-FISH analyses, were further validated by FISH experiments with locus-specific BAC probes. Interestingly, the long arm of the der(12) was shown to be almost entirely composed by amplified chromosome 12 sequences, together with chromosomes 7, 16 and 17 material (Fig. 4). Moreover, we finely mapped the breakpoints of all unbalanced translocations (data not shown). Then, combining classical cytogenetic, molecular cytogenetic and SNP array data for ANGM-CCS cell line, it was possible to define the karyotype as: 88~91,XXYY,-6,+7,+add(9)(p21.1)ishdup(5)(q34)x2,+der(8)t(8;10)(q24.2;q21.1),-10,+der(12)ishins(7;17;16)(12qter→12q24::7?::17?::16?::12q24.3)x2,+der(14)t(6;14)(p12;q11.2)x2,-17,+19,+20[cp32]. ANGM-CSS showed an increased expression of *EGFR* and *MET* as compared to a normal human astrocytes (NHA) cell line (data not shown). The relative mRNA expression value for the *MET* and *EGFR* in the tumor cell line was, respectively 4.65 and 1.45. ANGM-CSS did not show methylation of the *MGMT* promoter or pathogenic mutations in the hotspot regions (exons 5-8) of the *TP53* gene, neither were mutations detected in codons 12 and 13 of the *KRAS* gene. No *FIG-ROS1* or *FGFR3-TACC3* chimeric gene was detected. Six weeks after the subcutaneous injection of ANGM-CSS cells in athymic nude mice, all animals showed growth of a macroscopically visible tumor. Mice were sacrified eight weeks after injections and the tumors

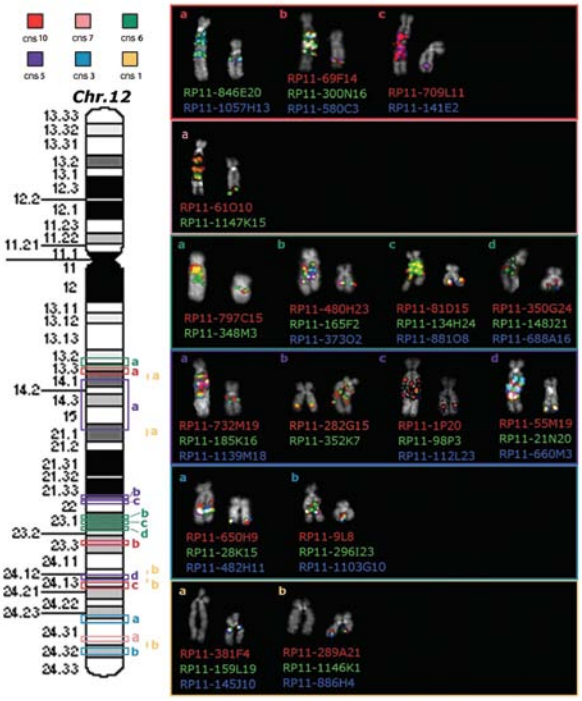

Figure 4. Map of the chromosome 12 locus-specific BAC probes used in FISH experiments (on the left) and partial metaphases showing the results obtained on both the normal and rearranged chromosomes 12 (on the right). Red, pink, green, violet and light blue rectangles on the chromosome 12 ideogram correspond to amplified sequences with copy number state (cns) of 10, 7, 6, 5 and 3, respectively. Conversely, yellow bars at the right side of the ideogram correspond to heterozygously deleted sequences, with cns of 1. Different chromosome 12 regions, with the same cns, are indicated, from the centromere to the telomere, by lowercase letters (a-d) in the same color. FISH results obtained with BAC probes, corresponding to each amplified/deleted region, are represented on the right side of the figure.

were immediately excised. One fragment was used for serial transplantation in other mice whereas the other section was used to start a new culture. The newly injected mice developed tumors two weeks after inoculation. The morphology of the cells grown after heterotransplantation did not differ from the initial culture (Fig. 1E). The human origin of the tumor cells was confirmed by chromosome analysis that revealed the same karyotype (data not shown).

Discussion

We successfully established a novel cell line, named ANGM-CSS, from a patient with GBM. Cell line immunoreactivity for GFAP showed a decrease after serial passages in culture, as previously described (23-27); whereas, the immunohistochemical positivity for vimentin and nestin was persistent. The immunohistochemical results recapitulate the phenotype of the GMB cell lines, according to data from literature (26-28). We provided a detailed characterization of ANGM-CSS by use of cytogenetic and molecular approaches. As expected, the cytogenetic analysis of ANGM-CSS showed a very complex karyotype characterized by several chromosome aberrations, in line with the data described in previous studies concerning human glioma cell lines (29-31). Gliomas have been extensively analyzed by genetic techniques. They typically show highly complex karyotypes (31). The most common numerical chromosomal changes include losses of 9p, chr10, chr17 and chr22 and gain of chromosomes chr7 and chr20 (31-35). Other structural abnormalities were also reported in chromosomal arms 1p, 6q, 9p, 9q and 13q (31). Similary to the latter data, G-banding, molecular cytogenetic and SNP array analysis performed on ANGM-CSS disclosed a near-tetraploid karyotype harbouring numerous copy number changes, including gain of whole chromosomes 7, 20 and 19 and loss of whole chromosomes 10, 14 and 21, in addition to gains of sub-regions in 5q, 7 and 17 and loss of 6q and 9p. Moreover, three structural chromosome rearrangements were identified in ANGM-CSS: a t(8;10)(q24.2;q21.1), a t(6;14)(p12;q11.2) and an add(9)(p21.1)ish dup(5)(q34). In summary, the genetic analyses indicate that the ANGM-CSS cell line recapitulates the key properties of GBM. The Cancer Genome Atlas Research Network reported in GBM frequent genetic alterations in three critical pathways: the RTK/RAS/PI3K, the p53 and the RB signalling pathways (36). ANGM-CSS presents a profound deregulation of proliferation and survival due to disruption of the RTK/RAS/PI3K pathway due to the amplification of the *EGFR* and *MET* genes and the homozygous deletion of *NF1* and *PTEN* genes, as detected by SNP array analysis (Table I). Quantitative RT-PCR analysis confirmed an increased expression at the mRNA level of the *EGFR* and *MET* genes. The cell line under study does not show the presence of *FIG-ROS1* and *FGFR3-TACC3* chimeric transcripts, already described for U118MG glioblastoma cell line and for primary tumors, respectively (19,20).

While no mutation or deletions were detected in the *TP53* gene, ANGM-CSS was characterized by amplification of the *MDM2* gene and homozygous deletion of the *CDKN2A* gene (Table I). The *MDM2* gene encodes for a protein involved in the degradation of the p53 protein and its expression is negatively regulated by the ARF protein, encoded by *CDKN2A*, leading to an abnormal regulation of apoptosis and senescence mediated by p53 (37). The Rb pathway was affected by the amplification of *CDK4* and *CDK6* and the homozygous deletion of the *CDKN2A*/*CDKN2B* genes. All these alterations affect the G1/S phase progression. Another feature of the ANGM-CSS is the absence of methylation in the promoter region of the *MGMT* gene. Alkylating agents induce cell death by forming cross-links between adjacent DNA strands through the alkylation of the O^6 position of guanine. *MGMT* promoter hypermethylation with consequent loss of MGMT protein expression reduces the DNA repair activity of glioma cells overcoming resistance to alkylating agents. The absence of *MGMT* promoter hypermethylation in ANGM-CSS leads to a transcriptionally active *MGMT* which rapidly removes the alkyl adducts preventing the formation of cross-links thereby causing resistance to alkylating drugs (38,39). ANGM-CSS cell also gave rise to tumors *in vivo*. All six SCID mice that were injected with tumor cells developed solid tumors, demonstrating that this cell line is capable of being propagated in animal models, which may aid in the development of test systems for new therapies.

Acknowledgements

This study was supported by Italian Health Ministry.

References

1. Furnari FB, Fenton T, Bachoo RM, *et al*: Malignant astrocytic glioma: genetics, biology, and paths to treatment. Genes Dev 21: 2683-26710, 2007.
2. Porter K, McCarthy B, Berbaum M, *et al*: Conditional survival of all primary brain tumor patients by age, behavior, and histology. Neuroepidemiology 36: 230-239, 2011.
3. Preusser M, de Ribaupierre S, Wöhrer A, *et al*: Current concepts and management of glioblastoma. Ann Neurol 70: 9-21, 2011.
4. Cheng L, Wu Q, Guryanova O, *et al*: Elevated invasive potential of glioblastoma stem cells. Biochem Biophys Res Commun 406: 643-648, 2011.
5. Louis DN, Ohgaki H, Wiestler OD, *et al*: The 2007 WHO classification of tumours of the central nervous system. Acta Neuropathol 114: 97-109, 2007.
6. Stupp R, Mason WP, van den Bent MJ, *et al*: Radiotherapy plus concomitant and adjuvant temozolomide for glioblastoma. N Engl J Med 352: 987-996, 2005.
7. Stupp R, Hegi ME, Mason WP, *et al*: Effects of radiotherapy with concomitant and adjuvant temozolomide versus radiotherapy alone on survival in glioblastoma in a randomised phase III study: 5-year analysis of the EORTC-NCIC trial. Lancet Oncol 10: 459-466, 2009.
8. Wen PY and Kesari S: Malignant gliomas in adults. N Engl J Med 359: 492-507, 2008.
9. Bakir A, Gezen F, Yildiz O, *et al*: Establishment and characterization of a human glioblastoma multiforme cell line. Cancer Genet Cytogenet 103: 46-51, 1998.
10. Nuki Y, Uchinokura S, Miyata S, *et al*: Establishment and characterization of a new human glioblastoma cell line, NYGM. Hum Cell 17: 145-150, 2004.
11. Wang J, Wang X, Jiang S, *et al*: Establishment of a new human glioblastoma multiforme cell line (WJ1) and its partial characterization. Cell Mol Neurobiol 27: 831-843, 2007.
12. Fomchenko EI and Holland EC: Mouse models of brain tumors and their applications in preclinical trials. Clin Cancer Res 12: 5288-5297, 2006.
13. Palumbo O, Palumbo P, Palladino T, *et al*: A novel deletion in 2q24.1q24.2 in a girl with mental retardation and generalized hypotonia: a case report. Mol Cytogenet 5: 1, 2012.
14. Macchia G, Trombetta D, Möller E, *et al*: FOSL1 as a candidate target gene for 11q12 rearrangements in desmoplastic fibroblastoma. Lab Invest 92: 735-743, 2012.

15. Scintu M, Vitale R, Prencipe M, *et al*: Genomic instability and increased expression of BUB1B and MAD2L1 genes in ductal breast carcinoma. Cancer Lett 254: 298-307, 2012.
16. Parrella P, la Torre A, Copetti M, *et al*: High specificity of quantitative methylation-specific PCR analysis for MGMT promoter hypermethylation detection in gliomas. J Biomed Biotechnol 2009: 531692, 2009.
17. Hibi K, Robinson CR, Booker S, *et al*: Molecular detection of genetic alterations in the serum of colorectal cancer patients. Cancer Res 58: 1405-1407, 1998.
18. Gu TL, Deng X, Huang F, *et al*: Survey of tyrosine kinase signaling reveals ROS kinase fusions in human cholangiocarcinoma. PLoS One 6: e15640, 2011.
19. Singh D, Chan JM, Zoppoli P, *et al*: Transforming fusions of FGFR and TACC genes in human glioblastoma. Science 337: 1231-1235, 2012.
20. Charest A, Lane K, McMahon K, *et al*: Fusion of FIG to the receptor tyrosine kinase ROS in a glioblastoma with an interstitial del(6)(q21q21). Genes Chromosomes Cancer 37: 58-71, 2003.
21. Burfeind P, Chernicky CL, Rininsland F, *et al*: Antisense RNA to the type I insulin-like growth factor receptor suppresses tumor growth and prevents invasion by rat prostate cancer cells in vivo. Proc Natl Acad Sci USA 93: 7263-7268, 1996.
22. Shaffer LG, Slovak ML and Campbell LJ (eds): ISCN 2009: An International System for Human Cytogenetic Nomenclature. S. Karger, Basel, 2009.
23. Lolait SJ, Harmer JH, Auteri G, *et al*: Expression of glial fibrillary acidic protein, actin, fibronectin and factor VIII antigen in human astrocytomas. Pathology 15: 373-378, 1983.
24. Lipsky RH and Silverman SJ: Effects of mycophenolic acid on detection of glial filaments in human and rat astrocytoma cultures. Cancer Res 47: 4900-4904, 1987.
25. Bocchini V, Casalone R, Collini P, *et al*: Changes in glial fibrillary acidic protein and karyotype during culturing of two cell lines established from human glioblastoma multiforme. Cell Tissue Res 265: 73-81, 1991.
26. Veselska R, Kuglik P, Cejpek P, *et al*: Nestin expression in the cell lines derived from glioblastoma multiforme. BMC Cancer 6: 32, 2003.
27. Jiang Y and Uhrbom L: On the origin of glioma. Ups J Med Sci 117: 113-121, 2012.
28. Krupkova O, Loja T, Zambo I, *et al*: Nestin expression in human tumors and tumor cell lines. Neoplasma 57: 291-298, 2010.
29. Bigner DD, Bigner SH, Ponten J, *et al*: Heterogeneity of Genotypic and phenotypic characteristics of fifteen permanent cell lines derived from human gliomas. J Neuropathol Exp Neurol 40: 201-229, 1981.
30. Roversi G, Pfundt R, Moroni RF, *et al*: Identification of novel genomic markers related to progression to glioblastoma through genomic profiling of 25 primary glioma cell lines. Oncogene 25: 1571-1583, 2006.
31. Dahlback HS, Brandal P, Meling TR, *et al*: Genomic aberrations in 80 cases of primary glioblastoma multiforme: Pathogenetic heterogeneity and putative cytogenetic pathways. Genes Chromosomes Cancer 48: 908-924, 2009.
32. Rey JA, Bello MJ, de Campos JM, *et al*: Chromosomal patterns in human malignant astrocytomas. Cancer Genet Cytogenet 29: 201-221, 1987.
33. Bigner SH, Mark J and Bigner DD: Cytogenetics of human brain tumors. Cancer Genet Cytogenet 47: 141-154, 1990.
34. Kruse CA, Mitchell DH, Kleinschmidt-DeMasters BK, *et al*: Characterization of a continuous human glioma cell line DBTRG-05MG: growth kinetics, karyotype, receptor expression, and tumor suppressor gene analyses. In Vitro Cell Dev Biol 28A: 609-614, 1992.
35. Gjerset RA, Fakhrai H, Shawler DL, *et al*: Characterization of a new human glioblastoma cell line that expresses mutant p53 and lacks activation of the PDGF pathway. In Vitro Cell Dev Biol Anim 31: 207-214, 1995.
36. Cancer Genome Atlas Research Network: Comprehensive genomic characterization defines human glioblastoma genes and core pathways. Nature 455: 1061-1068, 2008.
37. Uhrinova S, Uhrin D, Powers H, *et al*: Structure of free MDM2 N-terminal domain reveals conformational adjustments that accompany p53-binding. J Mol Biol 350: 587-598, 2005.
38. Esteller M, Garcia-Foncillas J, Andion E, *et al*: Inactivation of the DNA-repair gene MGMT and the clinical response of gliomas to alkylating agents. N Engl J Med 343: 1350-1354, 2000.
39. Hegi ME, Diserens AC, Gorlia T, *et al*: MGMT gene silencing and benefit from temozolomide in glioblastoma. N Engl J Med 352: 997-1003, 2005.